Reliable Adaptive Modulation and Interference Mitigation for Mobile Radio Slow Frequency Hopping Channels[1]

Ming Lei[+], Alexandra Duel-Hallen[+], Hans Hallen[*]

[+]North Carolina State University
Dept. of Electrical and Computer Engineering
Box 7911, Rayleigh, NC 27695-7911
Email: {mlei, sasha}@ncsu.edu

[*]North Carolina State University
Dept. of Physics
Box 8202, Rayleigh, NC 27695-8202
Email: Hans_Hallen@ncsu.edu

Abstract: Due to correlated fading in frequency hopping (FH) wireless communication systems, it is possible to predict the future channel state information (CSI) for one frequency based on past channel observations of other frequencies. This prediction capability enables adaptive transmission techniques for mobile radio FH systems. We investigate the optimal Minimum Mean Square Error (MMSE) Long Range Prediction (LRP) algorithm for slow frequency hopping (SFH) systems that employ coherent detection. A recursive filter update algorithm is proposed to reduce the complexity of this method. Statistical model of the prediction accuracy is developed and used in the design of reliable adaptive modulation techniques. Moreover, adaptive modulation is combined with adaptive transmitter frequency diversity to mitigate the effect of fading and partial-band interference in frequency hopping communications. Both standard Jakes model and a realistic non-stationary physical model are employed to test the performance. Analysis and simulation results show that significant performance gains can be achieved relative to non-adaptive methods.

Key words: Slow Frequency Hopping, Channel State Information, Long Range Prediction, Adaptive Transmission, Partial-band Interference, Diversity.

[1] This research was supported by NSF grant CCR-0312294 and ARO grants DAAD 19-01-1-0638 and W911NF-05-1-0311.

1. Introduction

In mobile wireless communications, system performance is severely degraded by rapidly time-variant multipath fading. Traditional communication systems designed for the worst-case channel conditions use a fixed link margin to maintain acceptable performance when the channel quality is poor, resulting in low bandwidth and power efficiency. Since high-speed data transmission is desired in future wireless communication systems, it is important to improve the bandwidth efficiency of mobile wireless communications while maintaining the low power constraint. To realize this goal, adaptation of the signal transmission to the fading channel conditions has been proposed.

Adaptive transmission techniques [1-4], such as adaptive power and rate control, adaptive modulation and coding, adaptive transmitter antenna diversity etc., have been investigated by many researchers. These adaptive transmission methods vary the transmission parameters according to the current fading conditions. Without sacrificing the Bit Error Rate (BER) performance, adaptive transmission provides high spectral efficiency by transmitting the signal at high rate during favorable channel conditions, and reducing the transmission rate when the channel conditions are poor. However, the performance of the adaptive transmission systems depends on the availability of the accurate Channel State Information (CSI). In most adaptive transmission systems, the CSI is estimated by the receiver and sent to the transmitter using a reliable feedback channel. Due to the delay associated with channel estimation and feedback, and the transmission format constraints, the CSI required at the time of transmission usually differs from the CSI estimated at the receiver. This outdated CSI is not sufficient for the adaptive transmission. For rapidly time-varying mobile radio channels, even a small delay will result in significant performance degradation. To realize the potential of adaptive transmission, it is necessary to predict the channel several milliseconds ahead.

A novel long range prediction (LRP) algorithm for the flat fading channel was proposed in [5-7] (see also references on fading channel prediction methods in [7,12,37-39]). This algorithm characterizes the fading channel using an autoregressive (AR) model and computes the Minimum Mean Square Error (MMSE) estimate of a future fading coefficient based on a number of past channel observations. Given fixed filter length, it benefits from using lower sampling rate than conventional techniques. This increases the memory span so that channel coefficients can be predicted further into the future. In [5-8, 14], the LRP algorithm for flat fading channel is applied in

adaptive power control, adaptive modulation and transmitter diversity for narrowband and direct sequence spread spectrum systems. It was demonstrated that LRP enables these adaptive transmission techniques for high vehicle speed and realistic feedback delays. In [12], the LRP is extended to Orthogonal Frequency Division Modulation (OFDM) channels, and in [11], LRP aided by observations at another carrier was investigated. Since variation of parameters associated with reflectors affects the prediction accuracy of LRP, a novel realistic physical model was developed to overcome the limitations of the standard Jakes model in testing our prediction algorithm [9,10]. Using this model, performance of adaptive transmission aided by LRP was validated in [7-9,11,12] for typical and challenging fading environments.

In this paper and [13,35], we explore adaptive transmission aided by the LRP for FH spread spectrum mobile radio systems that employ coherent detection. In FH communications [17], hopping provides frequency diversity and thus reduces the error probability due to deep fades. However, correlation of the fading between different frequency slots can be significant when the frequency separation is small compared to the coherence bandwidth of the channel [18]. This reduces the benefit of diversity. On the other hand, one can exploit the correlated fading at different frequencies in channel prediction. We propose to predict the channel coefficients in the next hopping frequency of slow frequency hopping (SFH) systems based on a number of past fading observations from previous hopping frequencies. An adaptive transmission method for SFH systems was previously investigated in [21,22], where a variable rate and power Reed-Solomon code was employed. The goal was to improve the throughput efficiency of the SFH systems by adapting to the slowly varying power of long term fading and the interference level. In this paper, we adapt the modulation level and the transmission power to rapidly varying short-term fading channel variations using the LRP for FH channels. The objective is to further increase the spectral efficiency subject to power and reliability constraints.

Partial-band interference also seriously degrades frequency hopping communication systems [17]. In practice, this kind of interference may be due to a partial-band jammer, or narrowband transmission in the same band as the FH signal. Coding is often used to mitigate the effects of partial-band interference in FH communications [17,21,22]. In [24], a pre-whitening filter was utilized to reject interference in the fast frequency hopping (FFH) receiver. Diversity combining techniques have also been proposed for the FFH systems with non-coherent detection [23]. In this paper, we investigate joint adaptive frequency diversity and adaptive modulation to mitigate the

effects of partial-band interference and fading in SFH systems with coherent detection.

The remainder of this paper is organized as follows. In section 2, we describe the system model and channel statistics. The MMSE Long Range Prediction algorithm for FH systems is introduced in section 3. In section 4, we analyze the performance of adaptive modulation aided by the LRP. This method is employed jointly with adaptive frequency diversity combining for SFH channels with partial-band interference in section 5. Numerical and simulation results are provided in both sections 4 and 5 to demonstrate the performance of adaptive transmission based on the LRP.

2. Channel Characteristics

Consider first the Frequency Selective Gaussian Wide Sense Stationary Uncorrelated Scattering (GWSSUS) channel model of the FH channel with q carrier frequencies [16]. Let $c(f(t),t)$ be the equivalent lowpass complex sample of the fading channel at time t and frequency $f(t)$, where $f(t)$ is the carrier frequency occupied at time t. To simplify notation, we use $c(f,t)$ instead of $c(f(t),t)$. We assume that fading is flat for each carrier frequency. The spaced-time spaced-frequency correlation function with the time difference τ and the frequency separation Δf is defined as [17]

$$R(\Delta f,\tau)=\mathrm{E}[c(f,t)c^{*}(f+\Delta f,t+\tau)] \tag{1}$$

From [16], the fading coefficients at frequency f^i can be expressed as

$$c(f^i,t)=\sum_{n=1}^{N}A_n e^{j(2\pi f_n t+\varphi_{in})} \tag{2}$$

where N is the number of reflectors. For the n^{th} path, A_n is the amplitude, and f_n is the Doppler shift. The phase difference for the n^{th} path between two frequencies f^i and f^j is $\Delta\varphi_n=\varphi_{jn}-\varphi_{in}=-2\pi\Delta f T_n$ [17], where $\Delta f=f^j-f^i$ is the frequency separation, and T_n is the excess delay of the n^{th} path, which is assumed to be exponentially distributed with the probability density function (pdf) [16]:

$$p(T)=\frac{1}{\sigma}e^{-T/\sigma} \tag{3}$$

where σ is the root mean square (rms) delay spread [18] of the multipath fading channel.

The channel coefficient $c(f,t)$ is closely approximated by a zero mean complex gaussian random process with Rayleigh distributed amplitude and uniformly distributed phase. The time correlation function of $c(f,t)$, defined as $R_t(\tau)=\mathrm{E}[c(f,t)c^{*}(f,t+\tau)]$, is given by [16]

$$R_t(\tau)=J_0(2\pi f_{dm}\tau) \tag{4}$$

where $J_0(\cdot)$ is a zero order Bessel function of the first kind and f_{dm} is the maximum Doppler shift.

The frequency correlation function $R_f(\Delta f)=\mathrm{E}[c(f,t)c^*(f+\Delta f,t)]$ is given by [11]

$$R_f(\Delta f) = \frac{1}{1+(2\pi\Delta f\sigma)^2} + \mathrm{j}\,\frac{2\pi\Delta f\sigma}{1+(2\pi\Delta f\sigma)^2} \tag{5}$$

Define $\Delta f\sigma$ to be the normalized frequency separation. From [29], $R(\Delta f,\tau) = R_t(\tau)R_f(\Delta f)$.

The deterministic Jakes model is often used to simulate the GWSSUS. This model employs time-invariant channel parameters (amplitudes, Doppler shifts and phases in (2)). While this model is sufficient in systems concerned with short-term channel behavior, it cannot adequately test the performance of the LRP method that employs long observation and prediction intervals. A novel physical model based on the method of images combined with diffraction theory was developed to generate more realistic fading datasets for testing the LRP [9,10]. In this paper, we employ the physical model in addition to the standard Jake model to validate performance of adaptive modulation aided by the LRP in FH channels.

3. Long Range Prediction for Frequency Hopping Channels

Consider the SFH system that employs coherent detection [19,20] with the total number of frequencies q and the hopping rate f_h. Denote the frequency separation between adjacent carrier frequencies as Δf. In this paper, we employ a randomly chosen periodic hopping pattern with length $N=q$, although the proposed methods also apply to non-periodic hopping patterns. Figure 1 illustrates the adaptive transmission aided by the LRP for this FH system. Past reliable observations from all frequencies are fed back from the receiver to the transmitter. The transmitter employs the LRP to predict future CSI, and adapts the transmission parameters to the channel variation.

We employ the MMSE linear prediction (LP) algorithm. Assume the channel coefficients in (2) are sampled at the rate $f_s=1/T_s$, and for an integer n, define $c(f(n),n)=c(f(nT_s),nT_s)$ in (2). The prediction $\hat{c}(f(n+\tau),n+\tau)$ (τ is a positive integer) of the future channel coefficient $c(f(n+\tau),n+\tau)$ based on p past observations $c(f(n),n),\ldots, c(f(n-p+1),n-p+1)$ is formed as (see figure 1b)

$$\hat{c}(f(n+\tau),n+\tau)=\sum_{j=0}^{p-1} d_j(n)c(f(n-j),n-j) \tag{6}$$

where $d_j(n)$ are the filter coefficients at time n, and τT_s is the prediction range. Note that the sampling rate in (6) is much slower than the symbol rate, but is faster than the hopping rate f_h.

The objective is to find the LP coefficients that minimize the Mean Square Error (MSE), defined as $E[|e(n)|^2]=E[|c(f(n+\tau),n+\tau)-\hat{c}(f(n+\tau),n+\tau)|^2]$. Because the hopping pattern is a random frequency sequence, a single prediction filter does not exist, and the LP coefficients need to be re-computed at the sampling rate. The LP filter used at sampling time n, denoted by $\boldsymbol{d}(n)$, is determined by the sampling time and the hopping pattern. The optimal prediction coefficients are computed as [17]

$$\boldsymbol{d}(n)=\boldsymbol{R}(n)^{-1}\boldsymbol{r}(n) \tag{7}$$

where $\boldsymbol{d}(n)=[d_0(n)\ldots d_{p-1}(n)]^T$, $\boldsymbol{R}(n)$ is the $p\times p$ autocorrelation matrix of the observations at time n with $R_{ij}(n)=E\{c(f(n-i),n-i)c^*(f(n-j),n-j)\}$, and $\boldsymbol{r}(n)$ is the cross-correlation vector of the observations and the prediction at time n given by $r_j(n)=E\{c(f(n+\tau),n+\tau)c^*(f(n-j),n-j)\}$, $i,j=0,1,\ldots,p-1$ for given τ. These functions are computed from (4, 5). In practice, noisy channel estimates are used in (6). The effect of the noise is incorporated into $\boldsymbol{R}(n)$ by adding $\sigma^2\boldsymbol{I}$, where σ^2 is the variance of the Gaussian estimation error, $\boldsymbol{I}$ is the $p\times p$ identity matrix; the vector $r_j(n)$ is also modified to include noisy observations [17,28].

The resulting instantaneous MMSE of this prediction method is [17]

$$\text{MMSE}(n)=1-\sum_{j=0}^{p-1} d_j(n)r_j(n) \tag{8}$$

The MMSE for FH systems is computed as the average over all LP filters $\text{MMSE}=\frac{1}{N}\sum_{n=1}^{N}\text{MMSE}(n)$.

When the channel is stationary and the channel correlation function (1) is known, the vector $\boldsymbol{d}(n)$ can be computed using (7). For realistic mobile radio channels, $R_t(\tau)$ and $R_f(\Delta f)$ in (5) must be estimated and updated when new observations are available. In our investigation, we use pilot symbols [29] to estimate these channel correlation functions. The estimate of the time correlation function is [30]:

$$R_t(\tau)=\frac{1}{N-\tau}\sum_{n=\tau}^{N-1} c(n)c^*(n-\tau), \quad \tau=0,1,2,\ldots, \tag{9}$$

where $c(n)$ are the pilot channel estimates at single frequency obtained at the sampling rate f_s, and N is the observation length.

The frequency correlation function can be estimated by inserting bursts of pilot symbols for

several frequencies at the symbol rate ($\tau_m \Delta F<1/2$, where τ_m is the maximum delay spread, and ΔF is the frequency separation between adjacent pilot channels [29]). The channel coefficients of other frequencies can be estimated by interpolation. Then frequency correlation function is estimated as

$$R_f(k\Delta f) = \frac{1}{M(N-k)} \sum_{i=1}^{N-k} \boldsymbol{c}^T(f^i)\boldsymbol{c}^*(f^{i+k}), \quad k=0,1,2,\ldots,N-1, \tag{10}$$

where M is the burst length (dwell interval in this paper), and $\boldsymbol{c}(f^i)=[c(f^i,j), c(f^i,j-1),\ldots,c(f^i,j-M+1)]^T$ is the vector of the estimated channel coefficients at frequency f^i at the symbol rate, i.e. $c(f^i,j)= c(f^i,jT)$, $1/T >> f_s$.

As new observations become available, R_{ij} and r_j in (7) are recomputed using the updated $R_t(\tau)$ and $R_f(k\Delta f)$, and $\boldsymbol{d}$ are updated. The required rate of update of the correlation functions depends on the rate of channel parameter variation. In this paper, the frequency correlation function is updated every 5-10 hops for the Doppler shift of 50Hz and the hopping rate of 500Hz. Moreover, the dependency of the adaptive modulation performance on the rate of update of the channel autocorrelation was analyzed in [11] for various rates of variation of the rms delay spread. It was demonstrated that much less frequent update rate is required, resulting in significant computational load reduction.

The optimal MMSE channel prediction method is complex, because it requires inversion of a large matrix at the sampling rate. The computation complexity is on the order of p^3 multiplications [41]. To reduce the computation, we observe that most elements in the autocorrelation matrix at time n can be obtained from the autocorrelation matrix at time $n-1$. This observation results in a procedure for updating the inverse of the autocorrelation matrix recursively [40] with the total number of multiplications on the order of p^2. Denote the autocorrelation matrices $\boldsymbol{R}(n-1)$ and $\boldsymbol{R}(n)$ as

$$\boldsymbol{R}(n-1)=\begin{bmatrix} \boldsymbol{R}_{(p-1)\times(p-1)}(n-1) & \boldsymbol{r}_{(p-1)\times 1}(n-1) \\ \boldsymbol{r}_{1\times(p-1)}(n-1) & r(n-1) \end{bmatrix}, \quad \boldsymbol{R}(n)=\begin{bmatrix} r(n) & \boldsymbol{r}_{1\times(p-1)}(n) \\ \boldsymbol{r}_{(p-1)\times 1}(n) & \boldsymbol{R}_{(p-1)\times(p-1)}(n) \end{bmatrix} \tag{11}$$

where $\boldsymbol{R}_{(p-1)\times(p-1)}(n) = \boldsymbol{R}_{(p-1)\times(p-1)}(n-1)$ and $\boldsymbol{r}_{1\times(p-1)}(n-1)=\boldsymbol{r}_{(p-1)\times 1}(n-1)^H$. The subscripts denote the dimensions of the submatrices, and the dimensions for scalars are not shown.

The algorithm for recursive update of $\boldsymbol{R}^{-1}(n)$ is as follows. Suppose the inverses at times $n-1$

and n are

$$\boldsymbol{R}(n\text{-}1)^{-1} = \begin{bmatrix} \boldsymbol{X}_{(p-1)\times(p-1)} & \boldsymbol{x}_{(p-1)\times 1} \\ \boldsymbol{x}_{1\times(p-1)} & x \end{bmatrix}, \boldsymbol{R}(n)^{-1} = \begin{bmatrix} y & \boldsymbol{y}_{1\times(p-1)} \\ \boldsymbol{y}_{(p-1)\times 1} & \boldsymbol{Y}_{(p-1)\times(p-1)} \end{bmatrix} \tag{12}$$

Then using the matrix inversion lemmas [25], we obtain $\boldsymbol{R}_{(p-1)\times(p-1)}(n)^{-1} = \boldsymbol{X}_{(p-1)\times(p-1)} - \boldsymbol{x}_{(p-1)\times 1}\boldsymbol{x}_{1\times(p-1)}/x$, and recursively compute the submatrices of $\boldsymbol{R}(n)^{-1}$ as:

$$\boldsymbol{Y}_{(p-1)\times(p-1)} = \boldsymbol{R}_{(p-1)\times(p-1)}(n)^{-1} - \frac{\boldsymbol{R}_{(p-1)\times(p-1)}(n)^{-1}\cdot\boldsymbol{r}_{(p-1)\times 1}(n)\cdot\boldsymbol{r}_{1\times(p-1)}(n)\cdot\boldsymbol{R}_{(p-1)\times(p-1)}(n)^{-1}}{\boldsymbol{r}_{1\times(p-1)}(n)\cdot\boldsymbol{R}_{(p-1)\times(p-1)}(n)^{-1}\cdot\boldsymbol{r}_{(p-1)\times 1}(n)-r(n)} \tag{13}$$

$$\boldsymbol{y}_{1\times(p-1)} = -\boldsymbol{r}_{1\times(p-1)}(n)\cdot\boldsymbol{Y}_{(p-1)\times(p-1)}/r(n),\ \ \boldsymbol{y}_{(p-1)\times 1} = \boldsymbol{y}_{1\times(p-1)}{}^{H} \tag{14}$$

and

$$y = 1/r(n) - \boldsymbol{y}_{1\times(p-1)}\cdot\boldsymbol{y}_{(p-1)\times 1}/r(n) \tag{15}$$

This procedure can be easily extended to noisy observations. Note that the proposed recursive procedure implements the original optimal MMSE method at reduced complexity. Thus, all numerical results in this paper are obtained using the proposed computationally efficient technique.

While it is possible to reduce complexity further by employing, e.g., the simplified LRP method in [13], we have observed that suboptimal LRP methods greatly degrade performance of adaptive FH systems. Therefore, we focus on the optimal MMSE prediction in the numerical results below.

To enable adaptive transmission in SFH systems, it is desirable to predict the channel coefficients for the next dwell interval using outdated observations in previous dwell intervals. Assume typical hopping rate of 500 hops/second, and feedback delay of at least 1ms. We found that the sampling rate f_s=2kHz results in the best performance for given parameters [15], so we employ this rate in further numerical examples. As a result, five samples are predicted for the upcoming dwell interval. (Since the sampling rate is much lower than the symbol rate [7], interpolation is performed within a dwell interval to predict fading coefficients for all data points [6]; the last predicted sample is outside the dwell interval and is used only for interpolation.) In our method, we employ computationally efficient method that utilizes the same matrix $\boldsymbol{R}(n)$ for all predicted samples within given dwell interval. Thus, to satisfy the feedback delay requirements, we employ the first two samples from the last dwell interval as the most recent observations ($j=0,1$ in (6)), and

vary τ to predict all five samples. This results in the average prediction range of τT_s=2ms. Figure 2 shows the MMSE vs. normalized frequency separation $\Delta f\sigma$ for various maximum Doppler shifts for this prediction range. We observe that the MMSE increases as the frequency separation grows, and the prediction accuracy degrades as the maximum Doppler shift increases. As the filter length p of the predictor increases, the MMSE decreases and saturates [6,11,15,36]. We employ $p=50$ in our examples since this value results in near-optimal performance [15]. The performance for different randomly chosen hopping patterns is also investigated [15]. It was observed that different hopping patterns with the same total bandwidth have similar performance. However, as the total bandwidth of FH systems increases, the prediction accuracy decreases [13].

In Figure 3, the degradation of the MMSE as the observation SNR decreases is illustrated. While the prediction MSE does not directly translate into the performance of adaptive transmission methods that employ prediction, in general the performance of adaptive transmission aided by the LRP is seriously degraded by realistic observation SNR values. Therefore, reliable channel estimation of the observed CSI is required. In this paper, we assume the effective SNR (after estimation) of 100dB. While the actual SNR of the observed samples might be much lower, noise reduction techniques can be employed to decrease the estimation error greatly [6,7,37-39]. Moreover, our investigation in [36] shows that bit rate degradation of adaptive modulation due to lower effective SNR values (e.g., 40 dB) is negligible. Therefore, accurate channel estimation assumed in this paper is realistic and is not a limiting factor in the performance of adaptive transmission enabled by the LRP.

4. Adaptive Transmission Aided by LRP

We employ variable rate variable power Multiple Quadrature Amplitude Modulation (MQAM) [1]. First, assume fixed transmission power E_s per symbol. The average Signal to Noise Ratio (SNR) is $\overline{\gamma}=E_s/N_0$, where N_0 is the power spectrum density of the equivalent lowpass complex additive white Gaussian noise (AWGN). The instantaneous SNR $\gamma=\overline{\gamma}\alpha(t)^2$, where $\alpha(t)=|c(f(t),t)|$ is the Rayleigh distributed channel amplitude [18]. The predicted channel amplitude $\hat{\alpha}=|\hat{c}(f(n),n)|$ is Rayleigh distributed [7].

In the adaptive modulation, the modulation level is adjusted according to the predicted channel amplitude to maintain the target bit error rate BER_{tg}. A decision rule for the modulation level

selection based on the prediction accuracy was investigated in [4,11]. Let $\hat{\alpha}$ be the predicted channel amplitude. The conditional pdf of α given $\hat{\alpha}$ is

$$p(\alpha|\hat{\alpha}) = \frac{2\alpha}{(1-\rho)\Omega} I_0\left(\frac{2\sqrt{\rho}\alpha\hat{\alpha}}{(1-\rho)\sqrt{\Omega\hat{\Omega}}}\right)\exp\left(-\frac{1}{(1-\rho)}\left(\frac{\alpha^2}{\Omega}+\frac{\rho\hat{\alpha}^2}{\hat{\Omega}}\right)\right) \tag{16}$$

where $\Omega=E[\alpha^2]$ and $\hat{\Omega}=E[\hat{\alpha}^2]$, and I_0 is the zero order modified Bessel function, and the correlation $\rho = \frac{\mathrm{cov}(\alpha^2,\hat{\alpha}^2)}{\sqrt{\mathrm{var}(\alpha^2)\mathrm{var}(\hat{\alpha}^2)}}$. The range of the channel amplitudes is divided into five fading regions by thresholds α_i, $i=1,\ldots,4$. For the predicted channel amplitude $\hat{\alpha}$, when $\alpha_i<\hat{\alpha}<\alpha_{i+1}$, M(i)-QAM is employed, where $M(1)=2$, $M(i)=2^{2(i-1)}$, $i=2,3,4$, $\alpha_5=\infty$. Given $\hat{\alpha}$, the average BER of the selected modulation level is

$$\mathrm{BER}_{M(i)}^{*}(\bar{\gamma},\hat{\alpha}) = \int_0^{\infty} \mathrm{BER}_{M(i)}(\bar{\gamma}\alpha^2)\, p(\alpha|\hat{\alpha})\mathrm{d}\alpha \tag{17}$$

where $\mathrm{BER}_{M(i)}$ is calculated using the upper bound of the BER of MQAM for AWGN channel [1]. The thresholds α_i are chosen as $\mathrm{BER}_{M(i)}^{*}(\bar{\gamma},\alpha_i)=\mathrm{BER}_{tg}$.

The performance of the fixed power MQAM can be improved by employing variable power. We extend the discrete power control policy [1] to the case where the observations are predicted, Once the thresholds are chosen as above, each modulation level is associated with a constant transmission power $E_s(i)$ selected to maintain the target BER. Assuming the ideal Nyquist signal, the spectral efficiency takes on the same value as the average number of bits per symbol (BPS):

$$R_{ada}=\sum_{i=1}^{4}\log_2 M(i)\int_{\alpha_i}^{\alpha_{i+1}} p_{\hat{\alpha}}(x)\mathrm{d}x \tag{18}$$

where $p_{\hat{\alpha}}(x)$ is Rayleigh distributed pdf. For the discrete power control policy, the actual average transmission power is:

$$P_{avg}=\sum_{i=1}^{4}E_s(i)\int_{\alpha_i}^{\alpha_{i+1}} p_{\hat{\alpha}}(x)\mathrm{d}x \tag{19}$$

The outage probability is given by

$$P_{out} = \int_0^{\alpha_1} p_{\hat{\alpha}}(x)\mathrm{d}x \tag{20}$$

We first use the standard Jakes model to validate the performance of the discrete power discrete rate adaptive MQAM described in this section. In the evaluation of the performance of SFH with adaptive modulation, the spectral efficiency is computed numerically using (18). When calculating the thresholds, the conditional pdf (16) is used in (17), and ρ is estimated by simulation. The following parameters are used in the simulations. The maximum Doppler shift is 50Hz. The frequency hopping rate is 500Hz. The channel sampling rate is 2KHz. A random hopping pattern with length 32 is employed. The filter length of the optimum MMSE prediction algorithm is 50. The symbol rate is 20Ksps (symbols per second). The modulation level is switched at the symbol rate. The target BER is 10^{-3}.

In figure 4, we plot BPS of the proposed adaptive modulation method vs. average SNR. We observe that significant gain can be achieved relative to the non-adaptive modulation. The gain depends on the normalized frequency separation. For example, if the normalized frequency separation is 0.05, the gain is 9-12 dB or 2-2.5BPS. If $\Delta f\sigma$ is smaller, greater gains can be achieved as illustrated in the figure. For $\Delta f\sigma$=0.01, the spectral efficiency with the MMSE prediction method is almost equal to the BPS with perfect CSI. For $\Delta f\sigma$=0.1, the gain relative to the non-adaptive modulation is about 3dB, or 1 BPS.

The BPS of adaptive modulation as a function of normalized frequency separation is shown in figure 5. We observe that the spectral efficiency of adaptive transmission degrades as $\Delta f\sigma$ increases. The FH system benefits from adaptive transmission primarily when $\Delta f\sigma$ does not significantly exceed 0.1. As $\Delta f\sigma$ grows, the spectral efficiency saturates and approaches that of non-adaptive modulation. Thus, adaptive transmission becomes less useful for greater normalized frequency separation, while the benefit of frequency diversity increases as $\Delta f\sigma$ grows.

Typical values of the delay spread are on the order of microseconds in outdoor radio channels [18]. Suppose σ is 1μs, representative of suburban areas. Then a SFH system would benefit from adaptive transmission when the frequency separation is as large as 100KHz ($\Delta f\sigma\approx$0.1). If σ is 10μs, the frequency separation has to decrease to 10kHz to obtain good performance. In realistic SFH systems [20], the symbol rate is on the order of tens of Ksps. Thus, the frequency separation of SFH

systems is often less than 100KHz. Therefore, adaptive transmission aided by the proposed channel prediction methods is feasible for these systems.

Note that as the number of frequencies q grows, the prediction accuracy decreases [13]. For example, we employ q=32 frequencies in our investigation. For this q, $\Delta f\sigma$ should not significantly exceed 0.1 to benefit from adaptive transmission. As q increases, lower $\Delta f\sigma$ is required for reliable performance. We have found that adaptive transmission is useful when the total normalized bandwidth ($q\Delta f\sigma$) is on the order of 3 or lower. In most SFH systems, the number of carriers is modest, i.e. q=32 is a typical value.

Next, we illustrate the dependency of the adaptive transmission for FH systems on the maximum Doppler shift f_{dm} in Figure 6. We observe that the performance gain is considerable when f_{dm} is moderate. However, for f_{dm} as large as 100Hz, the performance of the adaptive modulation systems is still better than the performance of the non-adaptive systems.

Finally, we use our physical model to investigate the performance of adaptive transmission in realistic non-stationary fading channels. In Figure 7, the average BPS vs. average SNR for the adaptive transmission in Jakes model and physical model is illustrated. A typical scenario and a challenging scenario are created to test the performance. The reflectors are arranged to give an approximately exponential distribution with the average rms delay spread σ=1μs for both scenarios [10]. The maximum Doppler shift is 50Hz. The frequency separation between adjacent frequencies is Δf=50kHz. Thus, $\Delta f\sigma\approx$0.05. In the typical case, the rms delay changes slowly, while in the challenging case, the rms delay changes rapidly in a wide range as shown in Figure 8. We use the method described in Section 3 to estimate and update the channel correlation functions. Since the channel correlation functions vary faster in the challenging scenario than in the typical scenario, the prediction accuracy is worse in the challenging case. While the BPS gain is lower for the physical model than for the Jakes model due to the channel parameter variations, significant improvement is still achieved relative to non-adaptive modulation.

In this paper, we employ frequently assumed exponentially distributed propagation delay as justified by [16]. Different distribution of the propagation delay will modify the frequency correlation $R_f(\Delta f\sigma)$. For example, for the uniform distribution, the coherence bandwidth and ρ will decrease for given σ, thus degrading the performance of the prediction and the bit rate relative to

the exponentially distributed excess delay. Since we directly estimate the frequency correlation $R_f(\Delta f\sigma)$ from the dataset, our algorithm is robust to the variation of the distribution of the propagation delay, as illustrated in the example above. Furthermore, performance of prediction for varying propagation delay parameters was analyzed in [11].

We observe significant loss in the bit rate of adaptive modulation aided by the LRP for FH channels relative to narrowband transmission [7,8,38], OFDM [12] and channels where observations are at a different frequency [11]. This loss is significant despite reduced maximum Doppler shift, and is further enhanced when our realistic physical model is employed rather than the Jakes model. For non-FH channels, the observations are at the same frequency, and thus much greater prediction accuracy is achieved, (in Fig. 7, the BPS is close to the "perfect CSI" curve for OFDM and narrowband cases, while the system in [11] results in only 0.5 BPS loss for 15dB.) Moreover, in non-FH channels, we can employ fast adaptive tracking combined with LRP to achieve almost the same prediction accuracy for the physical model as for the Jakes model. The reason why we have not achieved similar gains for FH systems is that the observations were constrained by the hopping pattern, and thus distributed in frequency. This constraint results in suboptimal sampling in frequency domain, and precludes utilization of fast adaptive tracking techniques.

5. Adaptive SFH Systems with Partial-band Interference

Partial-band interference (PBI) seriously degrades performance of frequency hopping communications [17]. In practice, this interference may be due to a jammer, or non-hostile out-of-system transmission. In our study, we are interested in the PBI that is not due to a hostile jammer, and therefore, does not vary rapidly [21,22]. The PBI is usually modeled as a narrow-band additive Gaussian noise. It occupies a small fraction δ of the total bandwidth of the FH system. For the frequency slots where PBI is present, the one-sided noise power spectral density is $N_0+\delta^{-1}N_I$, where N_I is the average power spectral density of the PBI. For the frequency slots without PBI, the one-sided noise power spectral density is N_0. We propose to use adaptive frequency diversity (referred to as diversity FH) to mitigate the effects of PBI. Since this method can also improve performance of SFH systems without PBI, we first describe the scheme in the interference-free case, and then extend to systems degraded by PBI.

In the proposed frequency diversity method, the same information is transmitted on two or

more carrier frequencies chosen according to a hopping pattern, and the outputs of different diversity branches are combined at the receiver using, e.g., selection combining (SC) or Maximal Ratio Combining (MRC) [17,23,27]. In the SC method, the receiver selects the output signal with the largest SNR, while in the MRC, signals from all frequencies are weighted prior to combining, with weights that are proportional to the SNRs of all frequencies. The MRC outperforms SC and is the optimal diversity combining method. As the number of diversity branches increases, the performance of both methods improves. This frequency diversity techniques can be combined with the adaptive modulation described in section 4. In this case, the channel gain in (17) is determined after diversity combining, thus improving on the gain of single Rayleigh fading channel. A similar combined Adaptive MQAM (AMQAM) and antenna diversity method was described in [14].

Now, consider the SFH with PBI. To reduce complexity, we employ diversity combining methods where only two frequencies are used for transmission. In practice, the hopping pattern should be designed to assure that these two hopping frequencies f^1 and f^2 have large frequency separation to reduce the frequency correlation. In this paper, we select the frequency f^1 first using the random hopping pattern. The other frequency f^2 is separated by half of the total bandwidth of the SFH system (given by $N\Delta f/2$) from f^1. For a typical normalized frequency separation $\Delta f\sigma$=0.05, the correlation between these two frequencies is only *0.04* (*N=32*). Note that significant diversity gain can still be achieved with correlation coefficient as large as *0.7*, with performance close to that of the independent fading case [26]. Thus, we can assume independent fading at the two hopping frequencies without affecting the performance significantly.

We assume that the receiver knows perfectly where the PBI is present. This can be achieved by estimating the noise power at the receiver [17,23]. At the transmitter, the two upcoming frequencies f^1 and f^2 can be monitored prior to the transmission [31,32] to determine if they have interference. Another method of predicting interference is based on Markov chain modeling [21]. Since the time variant nature of the interference induces uncertainty into this knowledge of the PBI, we introduce a reliability factor η to model the reliability of the prediction of the PBI at the transmitter. Let I_k denote the indicator function for the presence of interference at the upcoming frequency f^k:

$$I_k = \begin{cases} 1 & \text{interference is present at } f^k \\ 0 & \text{interference is absent at } f^k \end{cases}$$

Then the probability of the interference at the transmitter is modeled as

$$p_k = \eta I_k + (1-\eta)(1- I_k) \tag{21}$$

where $\eta \in [0,1]$. As η increases, the reliability improves. When $\eta=1$, the transmitter has perfect side information about the PBI.

The proposed combined adaptive modulation and adaptive transmission diversity method for the SFH systems operates as follows. According to a hopping pattern, symbols are transmitted on two frequencies simultaneously. At the receiver, diversity combining techniques described above [27] are employed to form the decision statistics. When there is no interference at both hopping frequencies, MRC is used by the receiver. When only one frequency has interference, the receiver employs Selective Combining (SC) to choose the frequency that does not have the interference. If both frequencies are interfered, we use random guess to detect data. This method has lower complexity and very similar performance to the optimal MRC conditioned on the interference and noise level [17].

Let f^1 and f^2 be the two hopping frequencies available for the next transmission according to the hopping pattern, and $\hat{\alpha}_1$ and $\hat{\alpha}_2$ be the predicted channel gains at f^1 and f^2, respectively. The average BER when $M(i)$-QAM is employed by the transmitter is

$$\begin{aligned} \mathrm{BER}_{M(i)}^{*}(E_s,N_0,\hat{\alpha}_1,\hat{\alpha}_2,p_1,p_2) &= (1-p_1)(1-p_2)\int_0^\infty\int_0^\infty \mathrm{BER}_{M(i)}\left(\gamma=\frac{E_s(\alpha_1^2+\alpha_2^2)}{N_0}\right)p(\alpha_1|\hat{\alpha}_1)p(\alpha_2|\hat{\alpha}_2)\mathrm{d}\alpha_1\mathrm{d}\alpha_2 \\ &+ p_2(1-p_1)\int_0^\infty \mathrm{BER}_{M(i)}\left(\gamma=\frac{E_s\alpha_1^2}{N_0}\right)p(\alpha_1|\hat{\alpha}_1)\mathrm{d}\alpha_1 + p_1(1-p_2)\int_0^\infty \mathrm{BER}_{M(i)}\left(\gamma=\frac{E_s\alpha_2^2}{N_0}\right)p(\alpha_2|\hat{\alpha}_2)\mathrm{d}\alpha_2 + 0.5p_1p_2 \end{aligned} \tag{22}$$

where $\mathrm{BER}_{M(i)}$ is derived as in (10), $p(\alpha_k|\hat{\alpha}_k)$ is the conditional pdf of α_k given $\hat{\alpha}_k$, and p_k is given by (21), $k=1,2$. Fixed power is employed, and the modulation level is chosen as

$$\tilde{M}=\max\{M(i) \mid \mathrm{BER}_{M(i)}^{*}(E_s,N_0,\hat{\alpha}_1,\hat{\alpha}_2, p_1,p_2) \le \mathrm{BER}_{\mathrm{tg}}\} \tag{23}$$

In the LRP for channels with PBI, past observations at interference-free dwell interval are used to form predictions about upcoming frequencies (f^1 and f^2). The optimal MMSE LRP algorithm with recursive autocorrelation matrix update is utilized. While PBI degrades the accuracy

of LRP, the quality of prediction is improved relative to interference free system without diversity [15].

Next, we describe a sentient frequency hopping diversity technique that can further improve the performance of SFH systems. In this method, channel coefficients of L widely spaced frequencies (selected according to the hopping pattern) are predicted, and a subset of r frequencies with the largest channel gains are selected in the transmission. The idea is similar to the selective transmitter diversity technique [14]. In the presence of PBI, the average BER for each modulation level is computed (e.g. for $r=2$, (22) is used, where f^1 and f^2 are the two frequencies with the largest prediction gains), and the largest signal constellation that satisfies the BER requirement is selected for the transmission. This method can be further improved by selecting r strongest frequencies that are not likely to be affected by interference.

While sentient FH has better performance than diversity frequency hopping due to its larger average channel gain, it is more complex, since greater number of frequencies has to be predicted. In practice, it is important to address the effects of these diversity methods on other users. While we predict a larger number (L) of frequencies in sentient FH relative to diversity FH, the actual transmission involves only a small number of frequencies (e.g. $r=2$), and lower average transmitted power. Thus, Multiple Access Interference (MAI) is reduced for sentient FH relative to diversity FH given the same number of transmitted frequencies.

Simulations are used to demonstrate the performance of adaptive SFH with PBI for typical values of δ ($\delta=0.1, 0.2$) [33]. The standard Jakes model is used. The adaptive modulation scheme described in section 4 is used with the modulation level selection given by (22, 23). In sentient FH, $L=4$ and $r=2$. We plot the average BER of diversity frequency hopping and sentient frequency hopping using adaptive modulation in Figure 9. The reliability factor $\eta = 0.98$, and the bandwidth of the PBI is $\delta = 0.1$. It is observed that the target $BER_{tg} = 10^{-3}$ is satisfied by the proposed adaptive modulation and diversity combining methods. In Figure 10, we plot the BPS performance of adaptive modulation using diversity FH and sentient FH under the assumption of perfect knowledge of PBI at the transmitter ($\eta=1$, $p_k=I_k$). As expected, the performance degrades as δ increases. The performance of sentient FH is better than that of diversity FH due to its larger channel gain. As L increases, the BPS of sentient FH saturates. Moreover, when L is very large, the BER actually increases due to prediction errors and the resulting inaccurate frequency selection. Our investigation

shows that $L=4$ has near-optimal performance [15].

In Fig. 10, we also illustrate the BPS of adaptive modulation for a non-diversity system (single Rayleigh fading channel) with PBI. In this case, adaptive modulation as in (17) is applied when the upcoming frequency is interference-free, and outage occurs if there is interference. Note that when this method is extended to $\eta<1$, the target BER cannot be satisfied, implying that diversity is required for channels with imperfect knowledge of PBI at the transmitter.

In Figure 11, we compare the outage probability of adaptive modulation for a single Rayleigh channel, diversity FH and sentient FH with PBI for $\eta=1$. It is observed that the outage probability of SFH systems can be greatly reduced by combining adaptive modulation with diversity techniques in the presence of PBI.

Figure 12 shows the BPS of adaptive diversity FH systems as a function of η. We observe that the spectral efficiency degrades as η decreases. For both diversity and sentient FH, when $\eta\leq 0.95$, the target BER cannot be satisfied with the adaptive transmission method proposed above. While this investigation is beyond the scope of this paper, we envision Adaptive Bit Interleave Code Modulation (ABICM) [34] as a suitable coding method for this application. Previously, ABICM has been shown to combine the benefits of adaptive transmission with those of time diversity of BICM techniques for flat Rayleigh fading channels. The adaptive TCM (ATCM) methods that do not utilize bit interleaving [2] require very high reliability of the CSI at the transmitter to achieve desired bit rate gains relative to non-adaptive TCM. In fact, when this reliability is high, ATCM techniques outperform ABICM methods, while ABICM achieves higher bit rates when the CSI becomes less accurate (e.g. due to unreliable prediction, challenging channel environment or low effective SNR). Moreover, ABICM can be implemented without the accurate statistical knowledge of the prediction error and thus is more robust than ATCM [34]. For systems with poor prediction of PBI as in Fig. 12, adaptive coded modulation schemes that utilize bit interleaving over several transmitted frequencies can provide additional diversity, similarly to non-adaptive coded techniques for combatting PBI [17]. The adavantages of this approach relative to ATCM without bit interleaving over frequencies will depend on the reliability of prediction of the fading and the PBI. These trade-offs and robustness of the ABICM for SFH systems with PBI can be subject of a future investigation.

6. Conclusion

Adaptive transmission is a powerful technique that improves the spectral efficiency of time-variant communication systems. Long Range Fading Prediction is crucial for adaptive transmission. The optimal MMSE channel prediction algorithm for SFH communications with coherent detection was introduced. A reduced complexity iterative matrix update method was proposed for this method. It was shown that for channel parameters that occur in practice, it is possible to predict the CSI of future frequency based on the channel observations of past frequencies. Both Jakes and realistic physical models were utilized in this investigation. It was demonstrated that the proposed LRP method enables adaptive modulation for SFH. Joint adaptive diversity combining and adaptive modulation was investigated for channels with PBI. Numerical and simulation results demonstrate that significant performance gains can be achieved relative to non-adaptive modulation for realistic FH systems.

References

[1] A.J. Goldsmith and S.G. Chua, "Variable-Rate Variable-Power MQAM for fading channels", IEEE Trans Comm, vol. 45, No. 10, Oct. 1997, pp. 1218-1230.

[2] A.J. Goldsmith and S.G. Chua, "Adaptive Coded Modulation for Fading Channels", IEEE Trans Comm, vol.46, No. 5, May 1998, pp. 595-601.

[3] T. Ue, S. Sampei, "Symbol Rate and Modulation Level-Controlled Adaptive Modulation/TDMA/TDD Systems for High-Bit-Rate Wireless Data Communicartion", IEEE Trans. Veh. Technol, vol.47, No.4, Nov. 1998, pp. 1134-1147.

[4] D. L. Goeckel, "Adaptive Coding for Time-Varying Channels using Outdated Channel Estimation", IEEE Trans. Comm., vol.47, No.6, June 1999.

[5] T. Eyceoz, A. Duel-Hallen, "Deterministic Channel Modeling and Long Range Prediction of Fast Fading Mobile Radio Channels", IEEE Comm Lett., vol.2, No.9, Sep. 1998, pp. 254-265.

[6] T. Eyceoz, S. Hu, A. Duel-Hallen, "Performance Analysis of Long Range Prediction for Fast Fading Channels", Proc. of 33rd Annual Conf. on Infom. Sciences and Systems CISS'99, March 1999, vol.II, pp. 656-661.

[7] A. Duel-Hallen, S. Hu, H. Hallen, "Long Range Prediction of Fading Signal: Enabling Adaptive Transmission for Mobile Radio Channels", IEEE Signal Processing Mag., vol.17, No.3, pp. 62-75,

May 2000.

[8] S. Hu, A. Duel-Hallen, H. Hallen, “Long Range Prediction Makes Adaptive Modulation Feasible for Realistic Mobile Radio Channels”, Proc. of 34rd Annual Conf. on Inform. Science, and Systems CISS’2000, Mar. 2000, vol. 1, pp. WP4-7 - WP4-13.

[9] H. Hallen, S. Hu, M. Lei, and A. Duel-Hallen, “A Physical Model for Wireless Channels to Understand and Test Long Range Prediction of Flat Fading”, Proc. of WIRELESS 2001, Calgary, July 9-11, 2001.

[10] H. Hallen, A. Duel-Hallen, S. Hu, T.S. Yang, M. Lei, “A Physical Model for Wireless Channels to Provide Insight for Long Range Prediction”, Proc. of MILCOM’02, Oct. 7-10, 2002.

[11] Tung-Sheng Yang, A. Duel-Hallen, H. Hallen, “Reliable Adaptive Modulation Aided by Observations of Another Fading Channel”, IEEE Trans. on Comm., vol. 52, No. 4, Apr. 2004, pp. 605-611.

[12] T.S. Yang, A. Duel-Hallen, H. Hallen, “Enabling Adaptive OFDM for Mobile Radio Channels”, Proc. of MILCOM’04, Oct. 2004, pp. 704-710.

[13] M. Lei, A. Duel-Hallen, “Long Range Channel Prediction and Adaptive Transmission for Frequency Hopping Communications”, Proc. of 41th Annual Allerton conference on Communication, Control, and Computing, Oct. 1-3, 2003.

[14] S. Hu, A. Duel-Hallen, “Combined Adaptive Modulation and Transmitter Diversity using Long Range Prediction for Flat Fading Mobile Radio Channels”, Proc. of IEEE GLOBECOM’2001, vol. 2, Nov. 2001, pp. 1256-1261.

[15] M. Lei, “Performance Analysis of Adaptive Slow Frequency Hopping Systems Aided by Long Range Prediction for Mobile Radio Channels”, Ph.D Dissertation, Fall 2004, http://www.ece.ncsu.edu/pubs/etd/id/etd-10272004-222632.

[16] W.C. Jakes, *Microwave Mobile Communications*. Wiley, New York, 1974.

[17] J.G. Proakis, *Digital Communications*. Fourth Edition, McGraw Hill, 1996.

[18] T.S. Rappaport, *Wireless Communications*: Principles and Practice. Prentice-Hall, 1996.

[19] S. Tomisato, K. Fukawa, and H. Suzuki, “Coherent Frequency Hopping Multiple Access

(CFHMA) with Multiuser Detection for Mobile Communication Systems", IEEE Trans. Vehi. Tech., vol. 49, Issue: 2, March 2000, pp. 531–539.

[20] M.P. Fitton, A.R. Nix, "Frequency Hopping CDMA for Flexible Third Generation Wireless Networks", Proc. of IEEE Global COM, 1997, vol.3, 3-8 Nov 1997, pp: 1504 –1508.

[21] M.B. Pursley, C.S. Wilkins, "Adaptive Transmission for Frequency-Hop Communications with Reed-Solomon Coding", IEEE Pacific Rim Conference on Communications, Computers and Signal Processing, vol. 2, 1997 pp. 866 –869.

[22] M.B. Pursley, C.S. Wilkins, "Adaptive-Rate Coding for Frequency-Hop Communication over Rayleigh Fading Channels", IEEE JSAC, vol.17, No.7, July 1999, pp. 1224-1232.

[23] C.M. Keller, M.B. Pursley, "Diversity Combining for Channels with Fading and Partial-Band Interference", IEEE JSAC, vol. SAC-5, No. 2, Feb. 1987. pp. 248-260.

[24] R.A. Iltis, J.A. Ritcey, L.B. Milstein, "Interference rejection in FFH systems using least square estimation techniques", IEEE Trans. on Comm., vol. 38, issue 12, Dec. 1990, pp.2174-2183.

[25] S. Haykin, *Adaptive Filter Theory.* Prentice-Hall, 1998.

[26] J.D. Gibson, *Principles of Mobile Communications.* Kluwer, 1996.

[27] D.G. Brennan, "Linear diversity combining techniques", Proc. of the IEEE, Vol. 91 Issue: 2, Feb. 2003, pp: 331 -356.

[28] Y. Li, L. J. Cimini, and N. R. Sollenberger, "Robust Channel Estimation for OFDM Systems with Rapid Dispersive Fading Channel," IEEE Trans. Commun., vol. 46, pp. 902-915, Apr. 1998.

[29] Y. Li, "Pilot Symbol Aided Channel Estimation for OFDM in Wireless Systems", IEEE Trans. on Veh. Tech., vol. 49, No. 4, July. 2000, pp. 1207-1215.

[30] M.H. Hayes, *Statistical Digital Signal Processing and Modeling*. John Wiley & Sons Inc., 1996.

[31] Gang Qiang; Zengji Liu; Susumu Ishihara; Tadanori Mizuno, "CDMA-based carrier sense multiple access protocol for Wireless LAN", VTC 2001 vol. 2, May 2001, pp: 1164-1168.

[32] O.C. Yue, R. Yeung, R.S. Bateman, S. Clark, "Performance of a frequency hopping CSMA packet radio network", Proc. of IEEE MILCOM 1990, vol.1, pp: 58 – 64.

[33]. T.J. Kumpumaki, M.A. Isohookana, J.K. Juntti, “Narrow-Band Interference Rejection using Transformation Domain Signal Processing in a Hybrid DS/FH Spread-Spectrum System”, Proc. of MILCOM 97, vol. 1, Nov. 2-5, 1997, pp. 89-93.

[34] P. Ormeci, X. Liu, D. L. Goeckel, and R. D. Wiesel, “Adaptive Bit-Interleaved Coded Modulation,” *IEEE Trans. on Comm*., Vol. 49, NO. 9, Sept. 2001, pp. 1572-1581.

[35] M. Lei, A. Duel-Hallen, “Enabling Adaptive Modulation and Interference Mitigation for Slow Frequency Hopping Communications”, proceeding of IEEE SPAWC 2005, June, 2005, pp. 366-370.

[36] T.-S. Yang, "Performance Analysis of Adaptive Transmission Aided by Long Range Channel Prediction for Realistic Single-and Multi-Carrier Mobile Radio Channels," Ph.D. Thesis,, NC State Univ, 2004, http://www.ece.ncsu.edu/pubs/etd/id/etd-05192004-133754.

[17] J. K. Hwang, J. H. Winters, “Sinusoidal Modeling and Prediction of Fast Fading Processes,” *Proc. IEEE Globecom’98*, Nov. 1998, pp. 892-897.

[38] S. Falahati, A. Svensson, T. Ekman, and M. Stenard, “Adaptive Modulation Systems for Predicted Wireless Channels.” *IEEE Trans. on Comm,*, Vol.52, No. 2, Feb. 2004.

[39] T. Ekman, “Prediction of Mobile Radio Channels: Modeling and Design”, PhD Dissertation, Uppsala University, Sweden, Oct. 2002.

[40] William H. Press, *Numerical Recipes in C : The Art of Scientific Computing*. Second Edition, 1992, Cambridge University Press.

[41] G. H. Golub, C. F. Van Loan, *Matrix Computations*. Third Edition, 1996, The Johns Hopkins University Press.

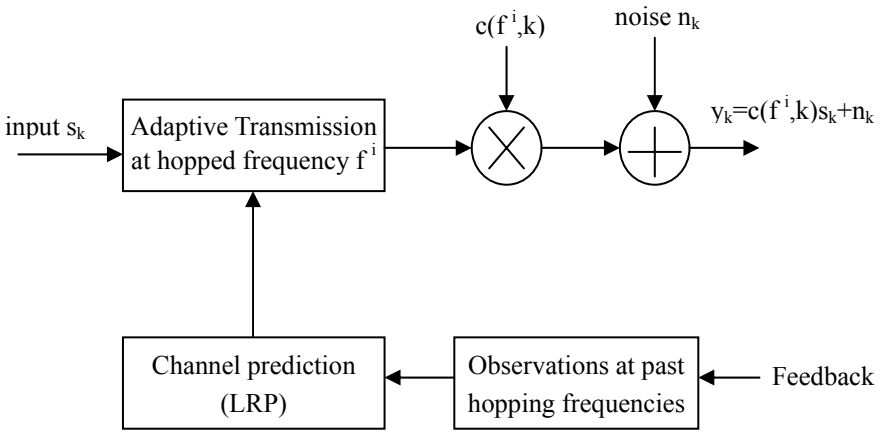

a. System model

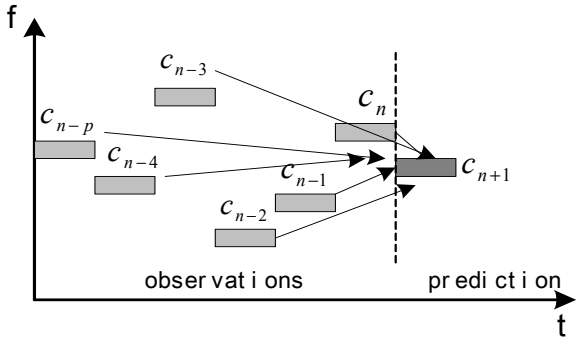

b. The LRP algorithm

Figure 1. Adaptive transmission for FH channels aided by long range prediction.

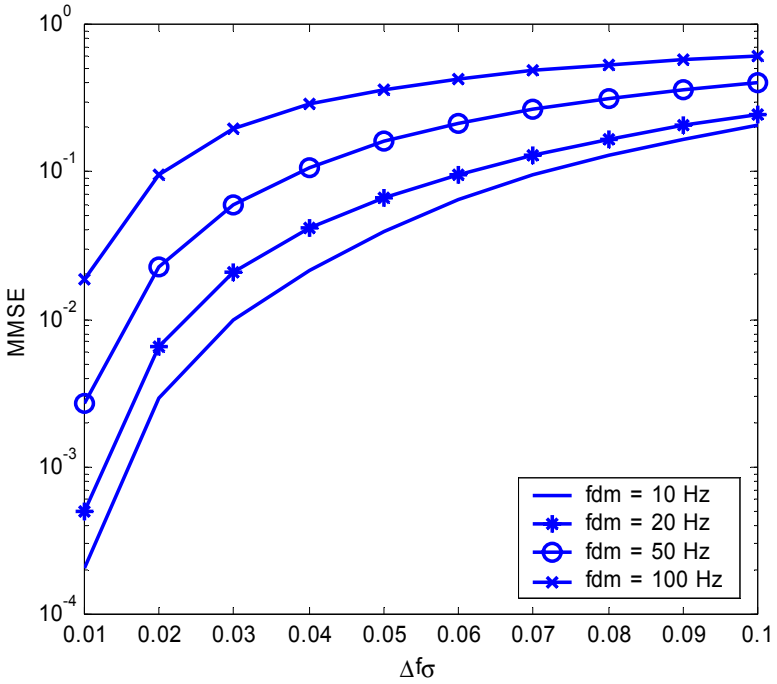

Figure 2. Performance of optimal MMSE LRP algorithm, $q=32$ and $f_s=2$KHz, $\tau T_s=2$ms, observation SNR=100dB.

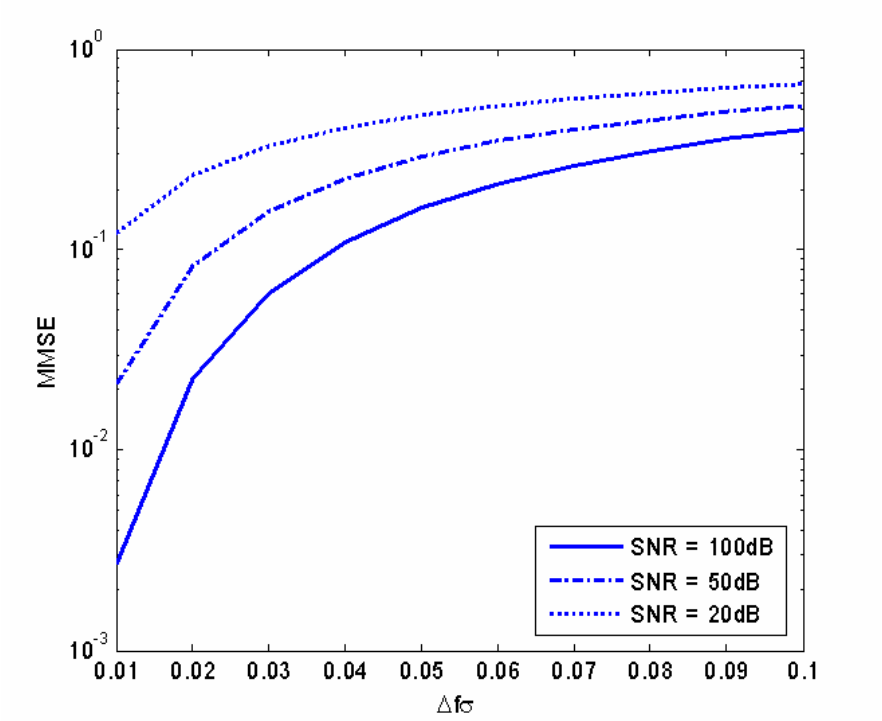

.Figure 3. Performance of optimal MMSE LRP algorithm for different observation SNR, $q=32$ and $f_s=2$KHz, $\tau T_s=2$ms, $f_{dm}=50$Hz.

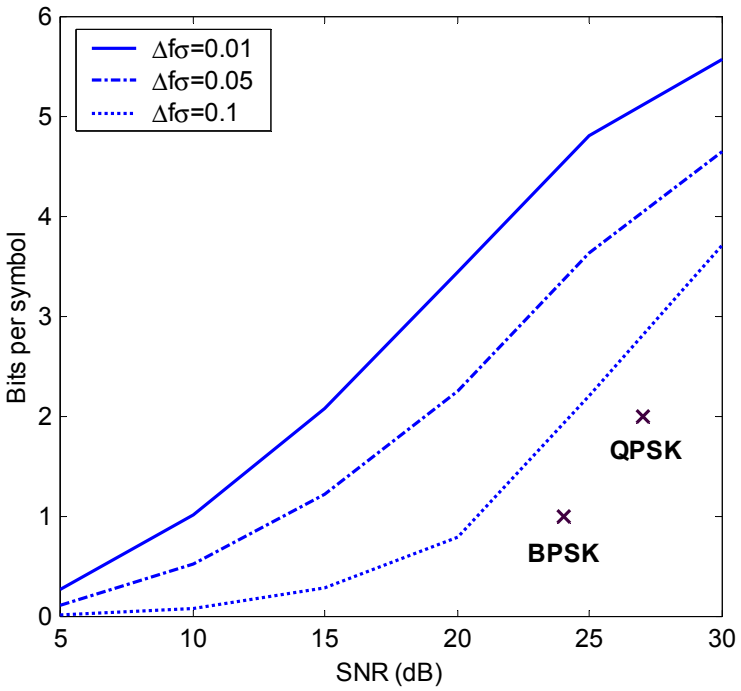

Figure 4. Spectral efficiency of adaptive modulation using Long Range Prediction,τT_s=*2*ms, f_{dm}=*50*Hz, *q=32*.

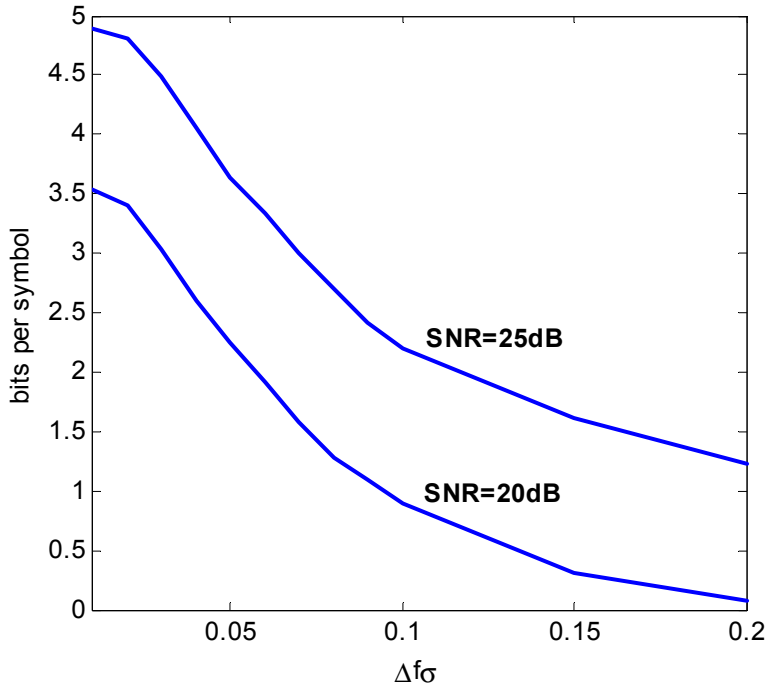

Figure 5. Spectral efficiency of adaptive modulation vs. $\Delta f\sigma$, $\tau T_s=2$ms, $f_{dm}=50$Hz, $q=32$, Jakes model.

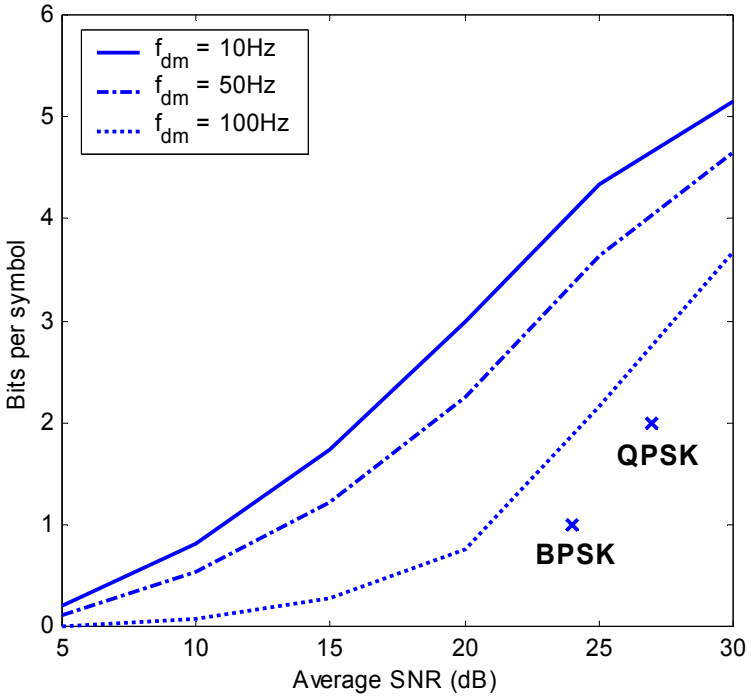

Figure 6. Spectral efficiency of adaptive modulation for different f_{dm}, $\Delta f\sigma = 0.05$, τT_s=2ms, q=32, Jakes model.

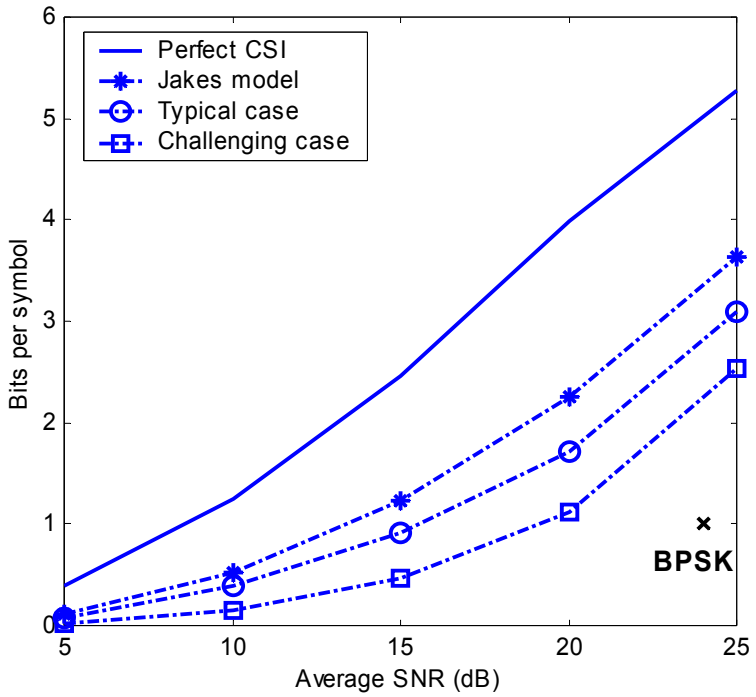

Figure 7. BPS vs. average SNR, average $\Delta f\sigma=0.05$, $q=32$, $\tau T_s=2$ms, $f_{dm}=50$Hz, $f_h=500$Hz, $f_s=2$kHz, $BER_{tg}=10^{-3}$.

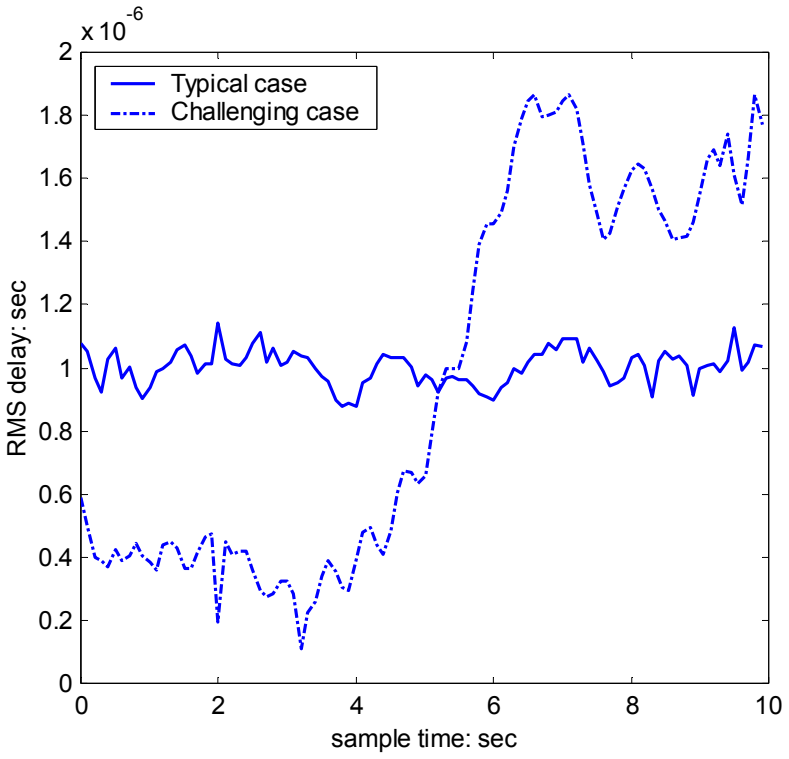

Figure 8. The variation of RMS delay σ in the typical and challenging cases.

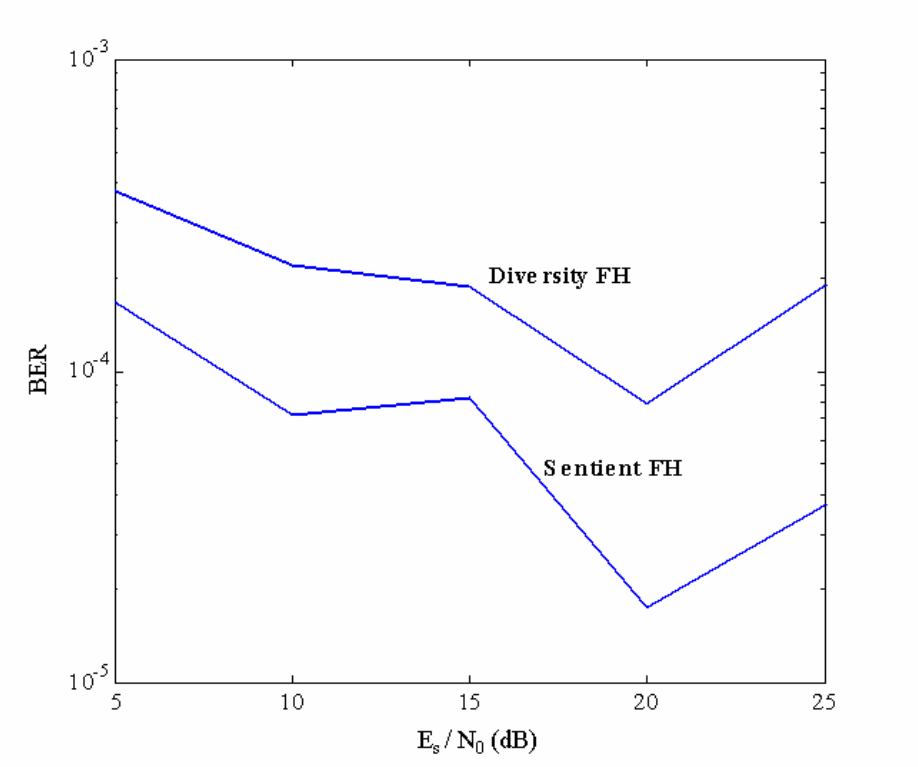

Figure 9. Average Bit Error Rate, $\eta = 0.98$, $\delta=0.1$, $\tau T_s=2$ms, $f_{dm}=50$Hz, $\Delta f\sigma=0.05$

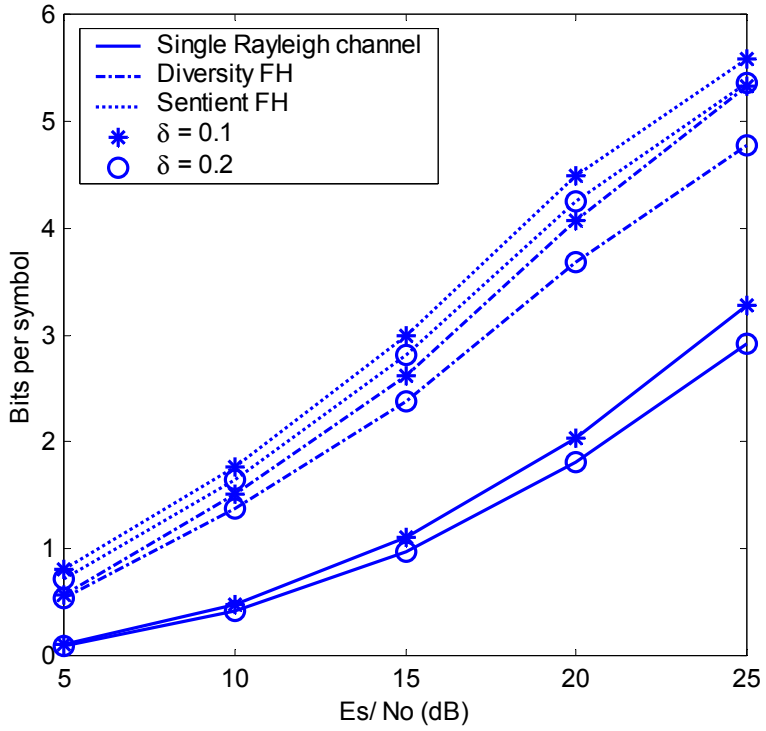

Figure 10. Performance of adaptive SFH with partial-band interference, Jakes model, τT_s=*2*ms, f_{dm}=*50*Hz, $\Delta f\sigma$=*0.05*, δ=*0.1*, η=*1.0*, *L*=*4*, *r*=*2* for sentient FH.

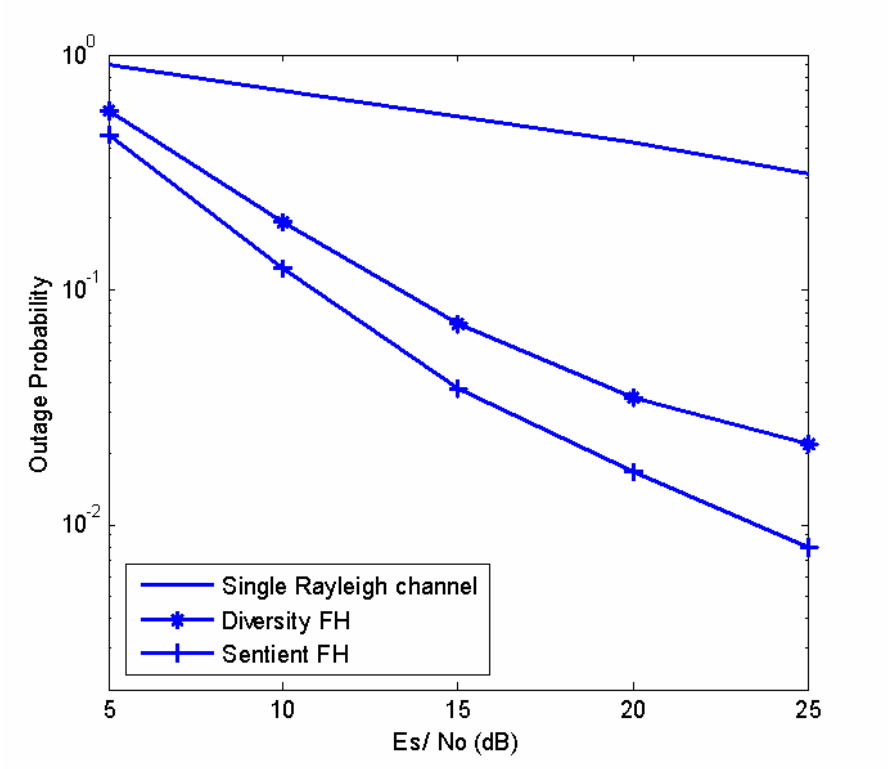

Figure 11. Comparison of outage probability, Jakes model, $\tau T_s=2$ms, $f_{dm}=50$Hz, $\Delta f\sigma=0.05$, $\delta=0.1$, $\eta=1.0$, $L=4$, $r=2$ for sentient FH.

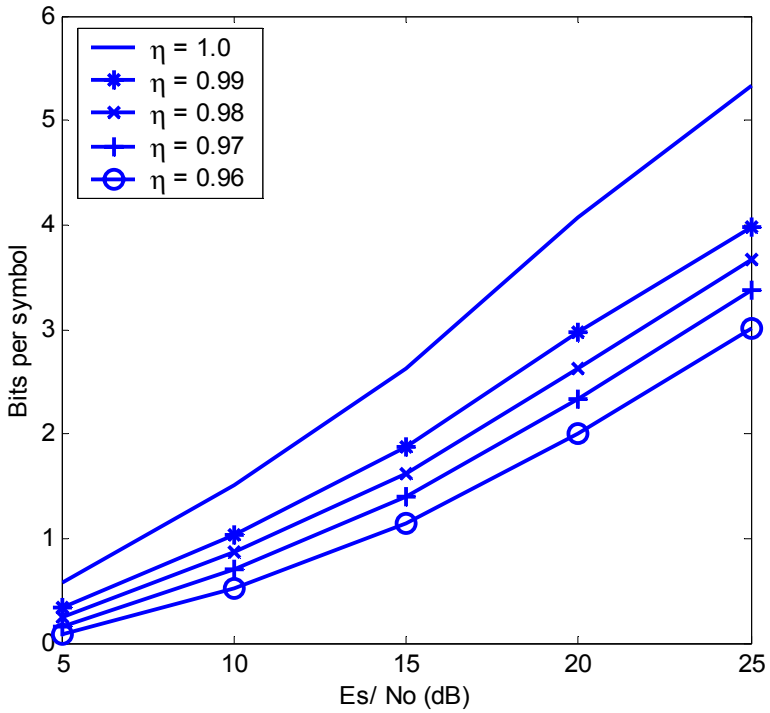

Figure 12. Performance of adaptive diversity FH with PBI, $\delta=0.1$, $\tau T_s=2$ms, $f_{dm}=50$Hz, $\Delta f\sigma=0.05$.